Applied Catalysis B: Environmental 134–135 (2013) 66–74

Contents lists available at SciVerse ScienceDirect

Applied Catalysis B: Environmental

journal homepage: www.elsevier.com/locate/apcatb

NO_X storage and reduction over a perovskite-based lean NO_X trap catalyst

Crystle Constantinou[a], Wei Li[b], Gongshin Qi[b], William S. Epling[a,*]

[a] Department of Chemical Engineering, University of Waterloo, Waterloo, Ontario, Canada
[b] General Motors Global R&D, Warren, MI, USA

ARTICLE INFO

Article history:
Received 11 September 2012
Received in revised form
27 December 2012
Accepted 29 December 2012
Available online 4 January 2013

Keywords:
NO_X reduction
NO_X trap
NO oxidation

ABSTRACT

Typical lean NO_X trap (LNT) catalysts contain Pt, which catalyzes NO oxidation and NO_X reduction, and an alkali or alkaline earth material for NO_X storage via nitrate formation. The catalyst is operated in a cyclic mode, with one phase of the cycle under oxidizing conditions where NO_X is trapped, and a second phase, which is reductant-rich relative to O_2, where stored NO_X is reduced to N_2. A recently developed catalyst uses a perovskite material as part of the LNT formulation for the oxidation reactions thereby eliminating the need for Pt. Pd and Rh are still added, to accommodate hydrocarbon oxidation and NO reduction, respectively. NO oxidation kinetics over the fully formulated and bare perovskite material were determined, with NO, O_2 and NO_2 orders being at or near 1, 1 and −1, respectively for both samples. The fully formulated sample, which contains Ba supported on the perovskite, was evaluated in terms of NO_X trapping ability and NO_X reduction as a function of temperature and reduction phase properties. Trapping and overall performance increased with temperature to 375 °C, primarily due to improved NO oxidation, as NO_2 is more readily trapped, or better diffusion of nitrates away from the initial trapping sites or into the Ba particles. At higher temperatures nitrate stability decreased, thus decreasing the trapping ability. At these higher temperatures, a more significant amount of unreduced NO_X formed during the reduction phase, primarily due to nitrate instability and decomposition and the relative rates of the NO_X and oxygen storage (OS) component reduction reactions. Most of the chemistry observed was similar to that observed over Pt-based LNT catalysts. However, there were some distinct differences, including a stronger nitrate diffusion resistance at low temperature, a more significant reductant-induced nitrate decomposition reaction and nitrate inhibition of OSC reduction at the onset of the regeneration phase.

1. Introduction

Traditionally, a three-way catalyst (TWC) has been used for gasoline engine exhaust clean-up, and is efficient in the removal and control of hydrocarbons (HC), CO and NO_X exhaust emissions. However for lean-burn engines, running with excess oxygen (such as diesel engines), the reduction of NO_X to N_2 is challenging and the TWC is not efficient enough to meet today's regulations. There has been significant research and development of lean-NO_X trap (LNT) catalysts [1–3] in response to the inherent challenge of reducing NO_X in an oxidizing environment.

LNT catalysts operate in a cyclic manner, with the gas composition shifting between the normally lean and an imposed rich atmosphere, and conventionally the catalyst formulation is $Pt/Ba/Al_2O_3$ [4]. The precious metal component is added for oxidation and reduction reactions and an alkali or alkaline-earth component to trap the NO_X on the surface as a nitrate. Research has shown that NO_2 is more effectively trapped than NO, and thus NO oxidation over the precious metal sites is a key reaction [5–9]. Eventually the catalyst needs to be regenerated to maintain its trapping ability (i.e. otherwise it will saturate and cannot trap NO_X further). During the regeneration portion of the cycle, the nitrates formed during the trapping phase decompose, NO_X species are released and migrate to reduction sites, and are finally reduced to N_2 [4]. This restores the surface for trapping.

As stated above, Pt is a standard LNT component, however Pt is quite costly. Researchers at General Motors have demonstrated that a perovskite-based catalyst, with no Pt, is efficient for NO_X trapping and reduction [10]. Perovskites would be an attractive alternative to Pt-based LNT catalysts, with their thermal stability and low cost. In the past, researchers have substituted different cations into the perovskite crystal lattice to tune catalytic capabilities for methane combustion, VOC combustion and NO_X storage and reduction [11–14]. The study performed by Kim et al. [10] included a comparison of different perovskite-based catalysts for diesel oxidation and lean NO_X trap catalyst performance. The study focused on NO_X trapping and reduction, NO to NO_2 conversion and sulfur poisoning. They observed that substituting Sr into La-based perovskites proved to be efficient in increasing surface area and acting as a structural promoter. López-Suáreza et al. have also studied

* Corresponding author. Tel.: +1 713 743 4234.
E-mail address: wsepling@uh.edu (W.S. Epling).

0926-3373/$ – see front matter © 2013 Elsevier B.V. All rights reserved.
http://dx.doi.org/10.1016/j.apcatb.2012.12.034

Table 1
Catalyst compositions. The perovskite sample described is the "fully formulated" sample used in the NSR studies. The perovskite material is $La_{0.9}Sr_{0.1}MnO_3$ [10]. The Umicore catalyst refers to the LNT catalyst studied in Ref. [19].

Catalyst	Pt	Pd	Rh	Ba	Ce	Zr
Perovskite	0	0.72	0.072	12	30	10
Umicore	1.5	0.4	0.16	6.2	30.4	2.3

Table 2
Kinetic study – experimental procedure and conditions.

Components	NO order test	O_2 order test	NO_2 order test	Ea test
NO	100–450 ppm	300 ppm	300 ppm	300 ppm
O_2	10%	4–12%	10%	10%
NO_2	170 ppm	170 ppm	80–180 ppm	170 ppm
Temperature	300 °C	300 °C	300 °C	240–320 °C

Sr-based perovskite LNT catalysts and showed good NO to NO_2 conversion and NO_X storage ability [14]. In the General Motors study, the $La_{1-x}Sr_xMnO_3$ (x = 0, 0.1) catalyst performed the best and was chosen as a good competitor for the Pt-based catalyst for LNT applications. In terms of oxidation performance, the perovskite catalyst had similar NO oxidation activity as a Pt-based catalyst tested. For example, at 300 °C, NO to NO_2 conversion was 86% for the perovskite-based catalyst, which was actually higher than the Pt-based catalyst studied at the same temperature. He et al. [15] also showed significant NO to NO_2 conversion and good NO_X trapping results on La-based perovskites.

Reference [10] also reported, however, that while the perovskites were comparable to the precious metal-based catalyst in terms of NO oxidation, for CO and hydrocarbon oxidation they did not perform as well. Pd, being active in CO and hydrocarbon oxidation [16], and much less expensive than Pt [17], was therefore added to the perovskite formulation [10]. This not only enhanced CO and hydrocarbon oxidation, but also the NO oxidation conversions noted, especially at low temperature. Another benefit of Pd addition is the possibility that Pd doping could significantly promote the thermal stability of the perovskite-based catalyst, as previously observed [18]. Via inclusion of some Rh (into a $La_{0.9}Sr_{0.1}MnO_3$-based LNT with precious metal loadings of 1.8 Pd/0.2 Rh ($g\,l^{-1}$)), the NO_X reduction capabilities were also comparable to the Pt-based catalyst. Overall, Ref. [10] concluded that there is significant potential for Pt-free perovskite catalysts as alternatives for the Pt-based catalysts in diesel aftertreatment catalysts, thereby reducing costs.

In this study, the $La_{0.9}Sr_{0.1}MnO_3$-based LNT catalyst, with precious metal loadings of 1.8 Pd/0.2 Rh ($g\,l^{-1}$) as described previously [10], was evaluated using a standard protocol developed by the Cross-Cut Lean Exhaust Emissions Reduction Simulations (CLEERS) group. This protocol was previously used to evaluate a commercial LNT (Pt-based) catalyst [19], with composition details listed in Table 1, and used here to investigate perovskite LNT chemistry and performance. The tests included NO_X storage ability, NO_X reduction efficiency, nitrite/nitrate stability as a function of temperature and NO vs. NO_2 as the NO_X source.

2. Experimental methods

The perovskite-based sample that was used in this study was provided by General Motors and the formulation is described in a previous paper [10]. The composition of the catalyst is detailed in Table 1. As a summary of its preparation, the $LaMnO_3$ was prepared by a citric acid method. $La(NO_3)_3{\cdot}6H_2O$ and $Mn(NO_3)_2$ (51% aqueous solution) were dissolved in distilled water together with citric acid monohydrate. The mixture was stirred for 1 h at 25 °C and then heated to 80 °C under continuous stirring. With heating, water was evaporated until the solution became a viscous gel and NO_X evolution was observed. The gel was then heated overnight at 90 °C. The resulting material was crushed and calcined at 700 °C for 5 h to form the perovskite part of the formulation. 4%Pd/Al_2O_3(Sasol), 2%Rh/CeO_2–ZrO_2 (Rhodia) and 20% BaO/Al_2O_3 were prepared using incipient wetness impregnation, with palladium nitrate, rhodium nitrate and barium acetate precursors. The samples were dried at 120 °C overnight and calcined at 550 °C for 5 h in air. The perovskite material was then ball-milled with the Pd/Al_2O_3, Rh/CeO_2–ZrO_2 and BaO/Al_2O_3 and the pH was maintained at 9.0 by adding aqueous ammonia solution. After ball milling for 18 h, the slurry was washcoated onto cordierite monolith core samples.

The sample had a 1.8 cm diameter and 2.6 cm length, and a 400 cpsi cell density. The sample was wrapped in a 3 M high temperature matting material to secure the sample in a quartz tube reactor and to prevent any gas bypass. The reactor tube was placed in a Lindberg/Blue Mini-Mite tube furnace to heat the sample. Two thermocouples were placed at the front and back faces of the catalyst in order to monitor and control the temperature. The feed gases, except balance N_2, were provided by PraxAir and metered to the reactor via Bronkhorst mass flow controllers. Balance N_2 was made via an OnSite N_2 Generator system. As H_2O was involved in most of the experiments, the tubing downstream of the mass flow controller manifold was heated to above 100 °C, and then H_2O was added to the gas mixture using a Bronkhorst CEM system.

For the NO oxidation kinetic study, NO_X storage and reduction cycling experiments, water gas shift (WGS), and oxygen storage capacity (OSC) experiments, the reactor outlet gases were monitored by a MKS MultiGas 2030 FTIR analyzer.

The NO oxidation kinetic study followed the same procedure laid out in Ref. [20] with the exception of the range of O_2 used, where only 6–14% was used here. The NO to NO_2 conversions were maintained near and below 10%. Reaction order experiments were run by varying one component concentration while holding the other components constant at 300 °C. All data points were taken when a steady state NO to NO_2 conversion was reached. To determine the activation energy, temperature was varied and data fit using the Arrhenius expression. Specific conditions are described in Table 2. Lastly the conditions under Ea test in Table 2 describe the experiment conducted in order to determine the activation energy. 95% confidence intervals are also listed.

In NO_X storage/reduction catalyst applications, a typical cycle consists of a lean phase of 1–2 min and a rich phase of 1–5 s. These "short" cycles were run in the process of this study, but longer duration cycles were also run, in order to more easily evaluate the chemistry occurring over the catalyst. For the short cycles, the catalyst was first cleaned/conditioned at 500 °C with 1% H_2, 10% CO_2, 10% H_2O and a balance of N_2, and then cooled to the target test temperature. Thirty cycles were then run. The lean phase lasted 60 s and was composed of 200 ppm NO, 10% O_2, 10% CO_2, 10% H_2O and a balance of N_2. The rich phase lasted 5 s and was composed of 1% H_2, 3% CO, 10% CO_2, 10% H_2O and a balance of N_2. The experiments were run at a 50,000 h^{-1} (STP) space velocity at 200, 300, 400 and 500 °C.

The long-cycle protocol was provided by the CLEERS group. The experiments performed were used to study the effect of temperature, the effect of NO_X source (NO or NO_2) and surface NO_X species decomposition either in the presence or absence of reductant. For the long cycles, the catalyst was first cleaned at 550 °C with 1% H_2, 5% CO_2, 5% H_2O and a balance of N_2, and then cooled to the target test temperature. Three reductant-present cycles were completed and then the 4th (last) cycle was run with no reductant in the rich phase. The lean phase lasted 15 min and was composed of 300 ppm NO or NO_2, 10% O_2, 5% CO_2, 5% H_2O and a balance of N_2. The rich phase lasted 10 min and was composed of 375 ppm H_2, 625 ppm

Table 3
CLEERS protocol – experimental procedure and conditions for long cycle experiments.

Run #	Temp	Gas mix	SV (h^{-1})	Lean period (s)	Reductant	Regen peak	Regen period (s)	# of cycles
1	550	1	30,000	0	H_2	1%	600	1
2	550	2/3	30,000	900	CO/H_2	1000 ppm	600	3
3	550	2/4	30,000	900	None	0	600	1
4	550	1	30,000	0	H_2	1%	600	1
5	463	2/3	30,000	900	CO/H_2	1000 ppm	600	3
6	463	2/4	30,000	900	None	0	600	1
7	550	1	30,000	0	H_2	1%	600	1
8	375	2/3	30,000	900	CO/H_2	1000 ppm	600	3
9	375	2/4	30,000	900	None	0	600	1
10	550	1	30,000	0	H_2	1%	600	1
11	288	2/3	30,000	900	CO/H_2	1000 ppm	600	3
12	288	2/4	30,000	900	None	0	600	1
13	550	1	30,000	0	H_2	1%	600	1
14	288	2A/3	30,000	900	CO/H_2	1000 ppm	600	3
15	288	2A/4	30,000	900	None	0	600	1
16	550	1	30,000	0	H_2	1%	600	1
17	200	2/3	30,000	900	CO/H_2	1000 ppm	600	3
18	200	2/4	30,000	900	None	0	600	1
19	550	1	30,000	0	H_2	1%	600	1
20	200	2A/3	30,000	900	CO/H_2	1000 ppm	600	3
21	200	2A/4	30,000	900	None	0	600	1

Inlet gas mix 1 = 5% H_2O, 5% CO_2, 1%H_2 and a balance of N_2; inlet gas mix 2 = 5% H_2O, 5% CO_2, 10% O_2, 300 ppm NO and a balance of N_2; inlet gas mix 2A = 5% H_2O, 5% CO_2, 10% O_2, 300 ppm NO_2 and a balance of N_2; inlet gas mix 3 = 5% H_2O, 5% CO_2, 625 ppm CO, 375 ppm H_2 and a balance of N_2; inlet gas mix 4 = 5% H_2O, 5% CO_2 and a balance of N_2.

CO, 5% CO_2, 5% H_2O and a balance of N_2. Specific conditions are described in Table 3.

3. Results and discussion

3.1. NO oxidation

Previous work has shown that NO_2 will absorb on LNT materials more efficiently than NO [5–9], which suggests that NO oxidation (NO to NO_2 conversion) is a critical step in improving the overall performance of a LNT catalyst. Pt-based catalysts have proven efficient and are commonly used; however similar trends and effective oxidizing capabilities with perovskite-based catalysts have been observed [10,13–15,18]. While NO_2 sorption increases the efficiency of the overall LNT catalyst performance, NO_2 itself inhibits NO oxidation over Pt-based catalysts [3,20]. It has been suggested that NO_2 absorbs easily to the oxidation sites, due to its high sticking coefficient [5,20,21], and oxidizes the Pt, thereby preventing NO adsorption and oxidation.

NO oxidation as a function of temperature data, over the fully formulated perovskite sample, are shown in Fig. 1. At low temperatures, low conversions were attained, due to kinetic limitations. NO to NO_2 conversion began to increase after 200 °C, increased until 350 °C, where the conversion began to drop due to thermodynamic limitations and the reaction then followed the equilibrium curve. In comparing these results to literature data, the same conversion trends are noted.

The NO oxidation kinetic behavior for the fully formulated perovskite-based sample was evaluated and the results are shown in Fig. 2. These NO oxidation experiments were conducted on a cleaned catalyst at 300 °C, with details listed in Table 2, and followed the procedure described in Ref. [20]. The rates were calculated and plotted against the respective varying component concentrations. The reaction orders for NO, O_2 and NO_2 were determined to be 1.13 ± 0.25, 1.06 ± 0.06, and -1.01 ± 0.26, respectively. These results are consistent with literature data for the conventional Pt-based catalyst [20] and a Pd-based catalyst [22], which suggests that the kinetic steps could be the same over the perovskite, Pt- and Pd-based catalysts.

A separate set of NO oxidation experiments was performed in order to determine the activation energy. The target temperatures were held constant until a steady-state NO to NO_2 conversion was achieved. Some previous activation energy (Ea) values found in literature data for the Pt/Al_2O_3 catalysts were 82 ± 9 kJ/mol as per Mulla et al. [20] and 75.9 kJ/mol as per Bhatia et al. [23], whereas

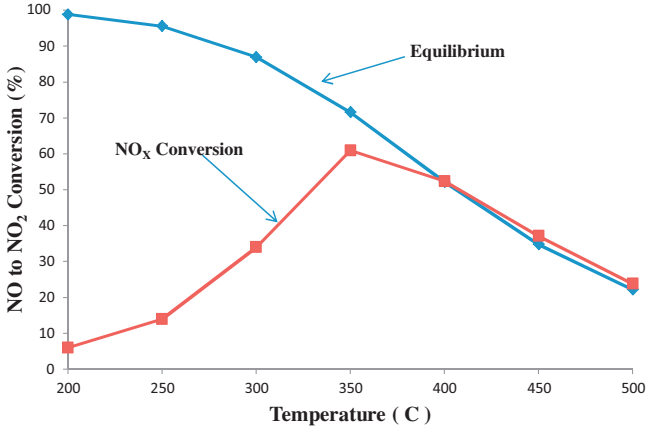

Fig. 1. NO oxidation as a function of temperature at 50,000 h^{-1} space velocity; 200 ppm NO, 10% O_2, 10% CO_2, 10% H_2O and a balance of N_2.

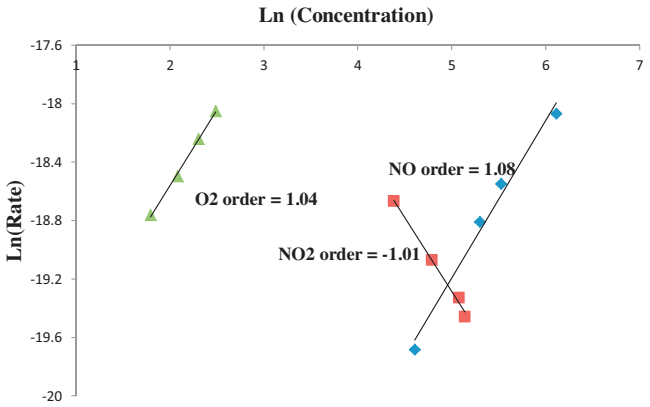

Fig. 2. NO oxidation rate vs. concentrations of NO, O_2 and NO_2; fully formulated perovskite. See Table 2 for inlet condition details.

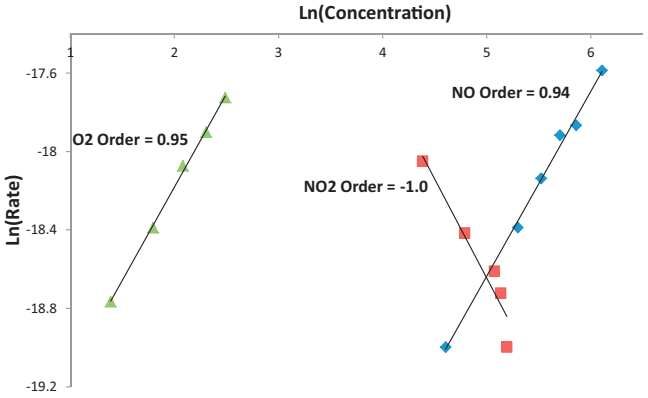

Fig. 3. NO oxidation rate vs. concentrations of NO, O_2 and NO_2; bare perovskite. See Table 2 for inlet condition details.

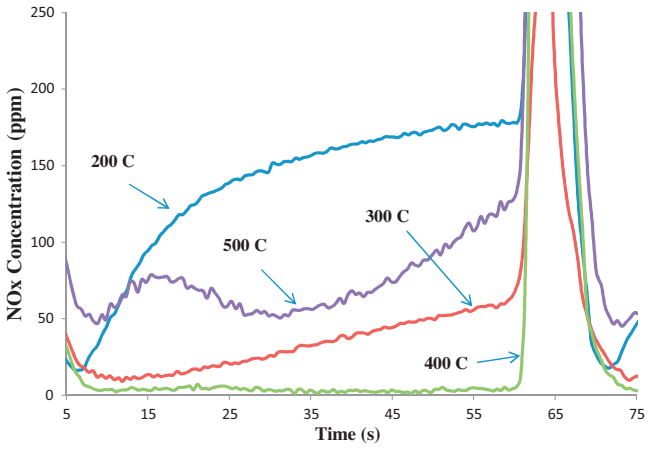

Fig. 4. NO_X ($NO + NO_2$) concentration profiles during cycling experiments for temperatures of 200, 300, 400 and 500 °C; 200 ppm NO, 10% O_2, 10% CO_2, 10% H_2O, balance N_2 at 50,000 h^{-1} space velocity.

Weiss and Iglesia [22] studied the NO oxidation reaction over a Pd/Al_2O_3 catalyst and reported an Ea of 152 kJ/mol. The catalyst used in our study contains Pd, but no Pt. The activation energy calculated for the fully formulated perovskite-based catalyst (containing Pd) was 82 ± 11 kJ/mol. The activation energy reported in Ref. [22] is much higher than the activation energy calculated using the perovskite-based sample, suggesting that the Pd itself does not play as much as of role in the reaction pathway, with the perovskite itself catalyzing the reaction. To qualitatively verify that Pd is not significantly contributing to the reaction pathway, the exact same NO oxidation experiments were completed on a bare perovskite sample (no precious metal included). The NO oxidation kinetic behavior for the bare perovskite-based sample was evaluated and the results are depicted in Fig. 3. The reaction rate orders were all found to be quite similar for NO, O_2 and NO_2; 0.94 ± 0.09, 0.95 ± 0.07 and −0.94 ± 0.29, respectfully. Furthermore, the activation energy over the bare perovskite sample was 81 ± 11 kJ/mol, which is still in the same range as the activation energy found in the fully formulated perovskite sample and previously tested Pt/Al_2O_3 samples [20,23]. The NO to NO_2 conversions over the bare perovskite, in the temperature range of the kinetics tests, were actually higher, but by only 2–3%, from 240 to 300 °C than those of the fully formulated sample. This demonstrates that the perovskite itself was indeed likely acting as the NO oxidation catalyst.

With the activation energies of the perovskite-based catalyst and the more traditional Pt-based catalysts being similar, a higher overall conversion over the perovskite-based sample would be expected since there is more total perovskite material. However, the active site on the perovskite is not known, leading to the likely possibility of some significant difference in the pre-exponential factors of the NO oxidation reaction over the two materials. When considering if it is the Mn or some active O species associated with the perovskite structure, this would decrease the level of active site concentration that may make the results more in line with an amount of exposed Pt. At this stage, however, it is unclear what is the active site on the perovskite, but apparently its concentration at the surface is not directly related to the bulk stoichiometry if considering the individual components.

3.2. NO_X storage and reduction

The storage or trapping ability of a LNT catalyst varies with temperature as does NO to NO_2 oxidation, a key step that goes hand-in-hand with the amount of NO_X stored. Past proposed trapping mechanisms involve NO_2 as the primary reactant for nitrate formation via the disproportionation reaction [3,19]. Also, Kwak et al. [24] have demonstrated that after NO_X begins to break through, the rate of uptake is determined by the gas/solid equilibrium between NO_2 and the available trapping sites. Thus more NO to NO_2 conversion will also affect the overall NO_X trapped. As shown in Fig. 1, at low temperatures NO oxidation is poor over the fully formulated perovskite-based catalyst due to kinetic limitations. Although sites are available and nitrates are more stable at lower temperatures, the lack of NO_2 formation will lead to poor storage. In general, as the temperature increases, NO oxidation extent also increases, but nitrate stability will decrease [19]. At higher temperatures the amount of NO_X trapped can therefore be limited by nitrate stability. Between 200 °C and 400 °C, significant NO to NO_2 conversion typically occurs (as depicted in Fig. 1) and the loss in nitrate stability is not significant, thus a maximum in NO_X storage is usually observed in this temperature range.

3.2.1. Short cycles

The short cycle storage profiles, shown as NO_X concentration as a function of time, at four different temperatures are shown in Fig. 4. Table 4 summarizes the data obtained during the short cycling experiments. The catalyst trapped the least amount of NO_X at the two temperature extremes, 200 and 500 °C, 14 and 22 μmol, respectively, with the onset of slip (NO_X breakthrough) occurring near the very beginning of the lean phase. At 200 °C, zero slip was not attained, with residual NO_X being released during the regeneration phase having to also be trapped at the onset of the lean phase. The best trapping performance was observed at 400 °C, with slip not observed during the lean phase. The amount of NO_X trapped increased from 200 to 400 °C, which follows the NO oxidation extent trend. The best overall NO_X conversion efficiency, 71%, was observed at 300 °C. At 400 and 500 °C, 58% and 9% were reduced, respectively, and at the lowest temperature, 200 °C, reduction was the lowest, 2%. In terms of the amount of stored NO_X that was reduced, only 4% was reduced at 200 °C, 87% at 300 °C, 64% at 400 °C (which is why overall conversion was better at 300 °C) and 18% at 500 °C.

In the 500 °C data set, there is a non-monotonic concentration change with respect to time. This pattern has been previously observed on a commercial LNT catalyst [25] and was attributed to a temperature wave moving through the catalyst, initially formed during the regeneration phase via exothermic oxidation reactions producing H_2O and CO_2. This heat generated was then conducted along the solid at a relatively slow rate and thus appeared during the lean phase. As the temperature increased, nitrates became more unstable, thus there was decreased trapping with the increase in solid temperature. This is what occurred at 500 °C over the perovskite sample as well.

Table 4
Short cycle storage and reduction performance results using NO as the NO_X source: 200 ppm NO, 10% O_2, 10% CO_2, 10% H_2O and a balance of N_2 in the lean phase (60 s); 3% CO, 1% H_2, 10% CO_2, 10% H_2O and a balance of N_2 in the rich phase (5 s).

Temperature (°C)	NO_X trapped (μmol)	NO_X released (μmol)	NO_X converted (μmol)	NO_X converted (%)	NH_3 formed (μmol)	N_2O formed (μmol)	N_2 formed (μmol)	NO_X converted (%) – using 4% H_2 as reductant
200	14	13.4	0.7	2	0.1	0.1	0.5	41
300	39	5	34	71	16	2	16	84
400	45	16	29	58	0	0	29	59
500	22	18	4	9	0.1	0.3	3.6	11

The same experiment was repeated with only H_2 as a reductant and even better conversion results were observed; overall NO_X conversions are also listed in Table 4. This is consistent with previous observations, where H_2 has proven to be a better reductant than a combination of CO and H_2 [26]. Again, the best overall conversion efficiency was observed at 300 °C, with a very significant gain at 200 °C obtained. The reason for the large gain at 200 °C is due to better reduction during the regeneration phase. As shown in Fig. 4, there are significant releases of NO_X during the regeneration phase, and the H_2 performed much better in reducing this released NO than the CO/H_2 mixture. This in turn resulted in better trapping as less NO_X originating from the regeneration phase needed to be "re-trapped" at the onset of the lean phase, thus contributing to the overall better performance observed. Overall, the results show that the perovskite LNT capabilities are good, especially at 300 and 400 °C. At higher temperatures, i.e. 500 °C, lower trapping and conversion values are due to the lack of nitrate stability. At lower temperatures, i.e. 200 °C, there is a much lower NO_X conversion likely due to poor NO oxidation and poor regeneration, though the latter is improved with decreased CO and/or increased H_2 as the reductant. When comparing the perovskite catalyst to a Pt-based catalyst with respect to short cycling, the trends appear the same [19,27]. In order to investigate the LNT chemistry further, long cycles were performed; that is longer time periods in the lean and rich phases.

3.2.2. Long cycles

The storage profiles, shown as NO_X concentration as a function of time, at five different temperatures are shown in Fig. 5. The plotted profiles are those of the third cycle of the protocol, by which time cycle-to-cycle stability was reached. Again, the catalyst trapped the least amount of NO_X at the two temperature extremes. 35 μmol of NO_X were trapped at 550 °C, with the onset of slip (NO_X breakthrough) at merely 4 s. At 200 °C, about the same amount was trapped and slip also began close to the beginning of the lean phase. A summary of the trapped amounts is listed in Table 5. The best trapping performance was observed at 375 °C, with 90 s elapsed prior to slip.

Ba is a common trapping component added to NSR catalysts, and was part of the perovskite catalyst formulation used in this study for this very reason. Previous research has shown that with Pt/Ba/Al_2O_3 catalysts, trapping performance decreases with increasing temperature above 375 °C due to decreasing nitrate stability [19,24]. The same trend at higher temperature was observed here, suggesting that the poor performance at high temperature was again due to low nitrate stability. Poor performance at lower temperatures can be attributed to poor trapping due to poor NO oxidation performance, slow NO_2 to nitrate formation; either via gas-phase desorption of NO_2 from an oxidation site then adsorption onto a trapping site or diffusion along the surface from the oxidation site to the trapping site or from the surface into the bulk of the Ba particles. This latter diffusion is the more likely of the two since the catalyst was prepared as a physical mixture, i.e. the Ba trapping site was deposited on Al_2O_3, which was them physically mixed with the perovskite. Another possibility is lack of regeneration, such that trapping sites became saturated after multiple cycles, which has been seen in previous work [28].

In order determine if it was regeneration or trapping performance, the first cycle (where the catalyst was previously cleaned and therefore NO_X-free) and the third cycle (where nitrate/nitrite build-up could have occurred if regeneration was limiting) were compared. As seen in Fig. 6, the first and third cycles overlap. If there was limited regeneration, then nitrates would build-up on the surface with each cycle. With such a build-up, the trapping performance would change between regenerations, which was not observed. This therefore demonstrates that it was not regeneration limiting the low temperature efficiency, but it was the trapping ability, which is consistent with the short cycling data where substantial NO_X release was observed during the regeneration phase.

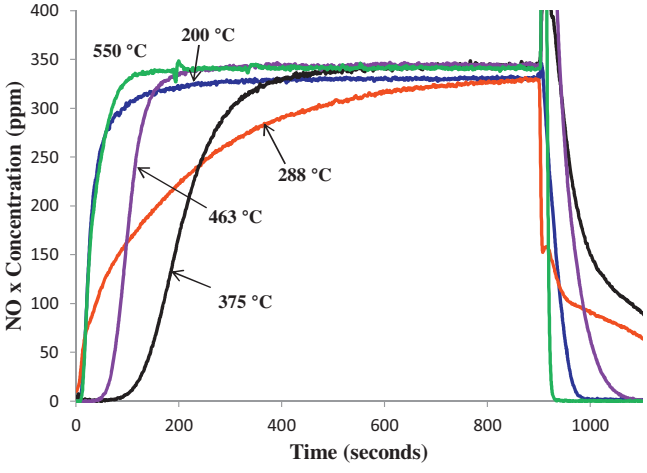

Fig. 5. NO_X ($NO + NO_2$) concentration profiles of third cycle during the storage period for temperatures 200, 288, 375, 463 and 550 °C; 300 ppm NO, 10% O_2, 5% CO_2, 5% H_2O, balance N_2 at 30,000 h^{-1} space velocity.

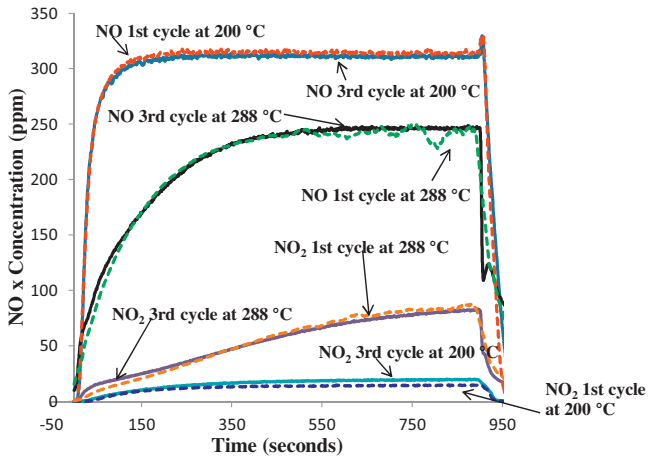

Fig. 6. 1st vs. 3rd cycles of NO_X storage at 200 °C and 288 °C. NO and NO_2 profiles shown. 300 ppm NO, 10% O_2, 5% CO_2, 5% H_2O, balance N_2 at 30,000 h^{-1} space velocity.

Table 5
Long cycle storage and reduction performance results using NO as the NO_X source: 300 ppm NO, 10% O_2, 5% CO_2, 5% H_2O and a balance of N_2 in the lean phase (15 min); 625 ppm CO, 375 ppm H_2, 5% CO_2, 5% H_2O and a balance of N_2 in the rich phase (10 min).

Temperature (°C)	Total NO_X trapped (μmol)	NO_X trapped (%) – at 20% BT	NO_X Released (μmol) – no reductant	NO_X released (μmol) – with reductant	NH_3 formed (μmol) – with reductant	N_2O formed (μmol)	N_2 formed (μmol)
200	36	21	27	28	11	0	0
288	137	56	36	70	44	3	17
375	188	92	119	136	30	0.44	22
463	93	55	90	90	0.1	0	3
550	35	18	32	33	0.07	0	2

NO_2 was still being formed and trapping sites were still available at these low temperatures. One cause for poor trapping can be slow nitrate formation from NO_2 or diffusion limitations as nitrates build up around the oxidation sites or from the surface of the Ba particles into the bulk. In previous Pt-based catalyst work similar diffusion limitations were noted [19,21], although at lower temperatures the overall NO_X conversion limitation was still attributed to a more significant effect of a lack of regeneration. In these previous studies, it was observed that even when reductant break through began there was leftover NO_X on the surface of the catalyst, confirming a limitation due to regeneration. In the case of the perovskite-based catalyst the limitation was due to trapping ability instead. One reason for this difference could be the lack of Pt, and its high sensitivity to CO poisoning during the regeneration phase. Previous LNT catalyst studies have shown that they are quite susceptible to CO poisoning at low temperature [26], and as Pd is less sensitive, this might explain the difference in low temperature limiting mechanism.

Table 5 summarizes the data obtained during the long cycling experiments and Figs. 7–9 are examples of the regeneration phase; NO, NO_2, N_2O, NH_3 and CO outlet concentration data as a function of time at different temperatures. The amount of NO_X trapped increased from 200 to 375 °C, which follows the NO oxidation extent trend again. In terms of the amount of NO_X trapped that was reduced during the regeneration phase, the best efficiency was observed at 288 °C, but still only 49% was reduced. At 375 °C and 200 °C, only 28% and 22% of the trapped NO_X were reduced, respectively, and at 463 and 550 °C reduction was quite poor. For example, at 550 °C the amount of NO_X released is very close to the amount trapped. At the higher temperatures this is in part due to a poor reduction rate relative to the nitrate decomposition rate. Similar trends were observed with a Pt-based commercial LNT catalyst [19] following the same CLEERS protocol as this study, where

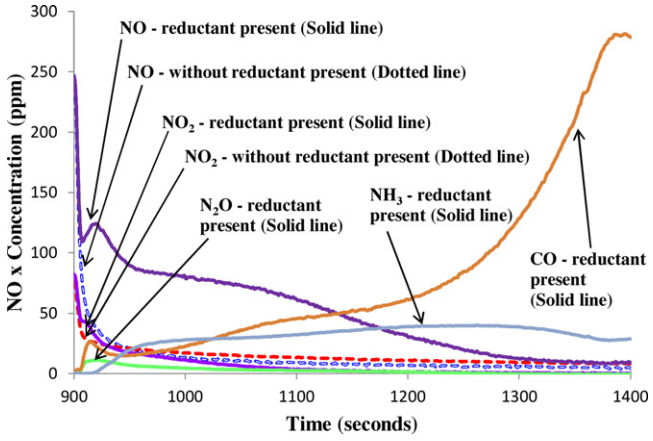

Fig. 8. NO (with and without reductant), NO_2 (with and without reductant), NH_3, N_2O and CO concentration profiles at 288 °C for the regeneration phase. With 625 ppm CO, 375 ppm H_2, 5% CO_2, 5% H_2O, balance N_2 at 30,000 h^{-1} space velocity.

incomplete reduction was observed at 550 and 463 °C. The authors concluded that there was a slower reductant delivery rate than the rate of nitrate decomposition and NO_X release. There was sufficient reductant delivery during the regeneration phase of the cycle taken as a whole. For example, Table 5 shows that at 550 °C, 35 μmol of NO_X were stored, so 87.5 μmol of reductant were needed for nitrate reduction. There was a 150 μmol/min reductant flux, so it should have taken just over half a minute for the stored NO_X to be reduced. However, as can be seen in Fig. 7, there was a sharp and rapid release of the stored NO_X (both with reductant and without reductant present) at the onset of the regeneration phase, and within several seconds release had ended. This confirms that the decomposition rate outpaced the reduction rate at this temperature. Complementing this observation, the data in Fig. 7 show no

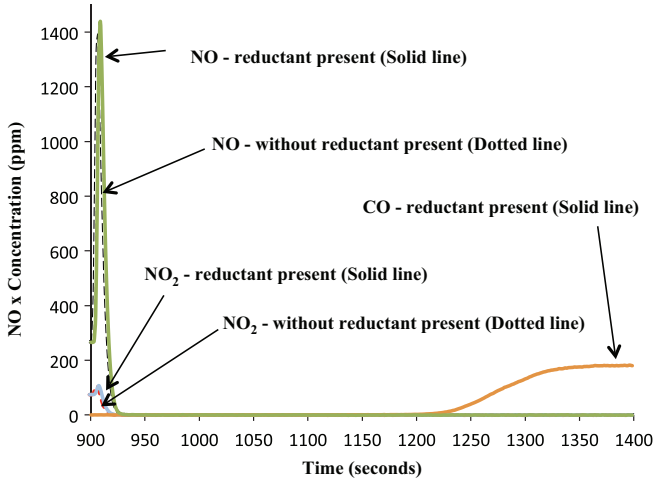

Fig. 7. NO (with and without reductant), NO_2 (with and without reductant), NH_3, N_2O and CO concentration profiles at 550 °C for the regeneration phase. With 625 ppm CO, 375 ppm H_2, 5% CO_2, 5% H_2O, balance N_2 at 30,000 h^{-1} space velocity.

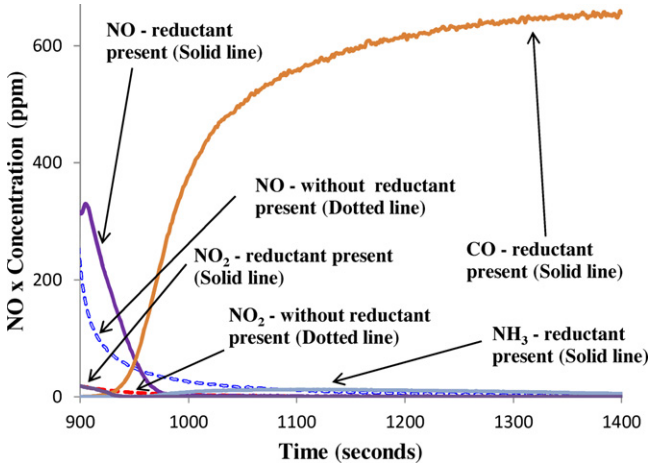

Fig. 9. NO (with and without reductant), NO_2 (with and without reductant), NH_3, N_2O and CO concentration profiles at 200 °C for the regeneration phase. With 625 ppm CO, 375 ppm H_2, 5% CO_2, 5% H_2O, balance N_2 at 30,000 h^{-1} space velocity.

difference between results when the reductant was present and absent – thus clearly nitrate decomposition dominates. Although there was no surface NO_X species reduction, there was significant reductant consumption, which must be related to reducing stored oxygen on the surface. Since the catalyst has measurable oxygen storage capacity (OSC), to be discussed below, competition arose between the stored oxygen and NO_X for the reductant. At 463 °C calculations of the amount of NO_X released and trapped also show little difference, for the same reasons. The release of NO_X at the outlet, via nitrate decomposition, was slower compared to 550 °C, but still quite rapid at the onset of the regeneration phase (data not shown for brevity). At both 463 and 550 °C, neither N_2O nor NH_3 was produced, as expected given the lack of NO_X reduction. These trends are consistent with the Pt-based catalyst studied previously [19].

The data listed in Table 5 show that at 200, 463 and 550 °C there was little to no difference in the amount of NO_X released when comparing the presence and absence of reductant during the regeneration phase. The reason for such at high temperatures was discussed above. As shown in Fig. 9, at 200 °C, reduction of stored nitrates occurs, with high selectivity to NH_3, when reductant was added. Without reductant, the amounts released were similar, but simply none was reduced, thus leading to the coincident amounts. The addition of reductant led to increased nitrate decomposition. At 288 and 375 °C, nitrate decomposition was not as rapid and therefore there were still nitrates on the surface that can be reduced by the reductants, as confirmed by the amount released with and without reductant present differing at 375 and 288 °C. With no reductant added, the nitrates still decompose thus resulting in some release.

At 375 °C, there was a much smaller NO_X "puff" at the onset of regeneration with reductant and no "puff" in the absence of reductant. The data obtained at 288 °C, shown in Fig. 8, show the same. These results demonstrate reductant induced nitrate decomposition, as was also observed at 200 °C, with more NO_X released at the beginning of the regeneration phase compared to that without reductant added. This effect was also seen on a model $Pt/Ba/Al_2O_3$ system by Nova et al. [29]. It should be noted that although reductant induced nitrate decomposition was demonstrated in this study there are other factors that affect nitrate stability. Nitrates and nitrites are less stable in the absence of O_2 [30], as in the regeneration phase, and also the presence of CO_2 has been seen to affect nitrates/nitrites stability [31].

Little to no N_2O was formed during the regeneration phase at any temperature. In terms of NH_3, at 375 °C, NH_3 release was observed after about 30 s from the onset of regeneration. The delay in the NH_3 observation can be attributed to a high NO_X to reductant ratio. Once the ratio begins to decrease, NH_3 formation becomes more favorable. The fact that NH_3 was still being released at the end of the regeneration phase shows that there was still some NO_X left on the surface. In testing Pt-based LNT catalysts, reductant breakthrough typically coincides with NH_3 observed [19]. Over the perovskite sample, an increase in CO concentration was observed at about the same time as NH_3, but CO breakthrough was also observed almost immediately after the onset of regeneration, rather than being delayed through reduction of OSC and nitrate consumption. Its concentration then decreased, before increasing again when NH_3 was also observed. These results suggest that surface NO_X species may be inhibiting CO reaction with OSC. At 288 °C, Fig. 8, CO was also observed at the onset of regeneration, and then the outlet concentration decreased, again indicating surface nitrates inhibit consumption of CO in OSC.

At 200 °C, there was some NH_3 formed during the regeneration phase and this amount increased at 288 °C and then decreased with increasing temperature. When NH_3 was produced, it was observed when the reductant concentration began to increase, as shown in Figs. 8 and 9, beyond the initial slip peak due to OSC reduction inhibition, and in addition there must have been leftover NO_X on the surface of the catalyst since NH_3 formation was still observed at the end of the regeneration phase. This was again also seen in previous research with a Pt-based LNT catalyst [19]. It has been proposed that H_2 can react with either OSC or surface NO_X, and therefore when no more OSC is being reduced, the H_2 can react selectively with either NO or other surface N-species to form NH_3 [32]. Furthermore, since there is no more OSC, NH_3 is therefore observed in the outlet, i.e. NH_3 is not also consumed in reducing stored oxygen. Over the perovskite sample, the fact that NH_3 was formed at or after CO breakthrough (so little to no OSC was being reduced) and after NO_X was no longer being released supports such a mechanism. Previous research has also shown that NH_3 formation is dependent on the reductant to stored NO_X ratio [33]. The higher the ratio, the more NH_3 is formed. The data shown here follow the same trend. As the stored NO_X was reduced, less was present and thus deeper reduction was observed. Furthermore, NH_3 is a known reductant in NSR chemistry. It is able to reduce stored nitrates [34,35]. Thus, as the amount of stored NO_X decreased, less NH_3 was consumed via NO_X reduction and was therefore observed. At a device/integral level, it is formed at upstream sites early during the regeneration phase [26], but is consumed at downstream sites where stored NO_X still exists. Once these are consumed, NH_3 is observed. All of these are consistent with the overall higher reductant-to-NO_X ratio leading to more NH_3 generation. At higher temperatures, where nitrate decomposition is rapid, less stored NO_X is available to react with the reductant and thus less NH_3 is formed.

In all, most of the trends are similar to those observed over a Pt-based LNT catalyst, where a decrease in temperature led to a decrease in the amount of NO_X released relative to the amount of NO_X trapped. For both catalysts trapping was limited by both NO oxidation and/or nitrate formation and diffusion at lower temperatures. It should be noted that NO_2 gas-to-solid phase equilibrium may also limit the total trapped as will be discussed in more detail below, but this is directly related to NO oxidation, as NO_2 must first be formed for this limitation to play a role. Furthermore, the preparation method does not include direct impregnation of the Ba trapping component onto the perovskite. The Ba is deposited on a CeO_2/ZrO_2 material which is then mixed with the perovskite and the physical mixture ball-milled together. At higher temperatures both catalysts are limited by nitrate stability. NH_3 formation was observed with reductant breakthrough or high reductant to stored NO_X ratios. There was a substantially higher level of NO_X conversion during short cycling than long cycling in the moderate operating temperature region. Short cycling led to better overall conversions due to more reductant readily available for reduction relative to all initially being consumed for OSC reduction, as well as less NO_X stored during the shorter lean phase.

However, there were some differences noted. At lower temperatures, the perovskite still did not perform as well suggesting a diffusion limitation that is stronger on the perovskite than that of the Pt catalyst or that the lower NO_2 concentrations at lower temperatures have a more dramatic effect on trapping, i.e. the NO_2 gas-to-solid phase equilibrium, which would include the diffusion of the nitrate from the Ba surface into the bulk, with more NO_2 creating a larger driving force, is critical for the perovskite-based catalyst. Furthermore, low temperature trapping performance was not limited by regeneration, but by slow NO_2 adsorption and nitrate formation possibly in conjunction with this diffusion or NO_2 equilibrium limitation. Another difference was the amount of NO_X released in the presence and absence of reductant, where the perovskite demonstrated a stronger dependence on reductant induced nitrate decomposition than that observed with the Pt-based sample [19]. Furthermore, there was immediate breakthrough of reductant, i.e. at the onset of the regeneration phase, at 288 and 375 °C,

Table 6
Amount of O_2 stored and WGS extents at 200, 288, 375, 463, 550 °C.

Temperature (°C)	O_2 stored (mmol)	WGS extent (%)
200	0.06	3
288	0.11	55
375	0.31	*
463	0.41	85
550	0.44	70

* not measured.

indicating that nitrates may inhibit OSC reduction via reductant consumption.

3.3. Water gas shift (WGS) extent

Water gas shift (WGS) is a common reaction occurring during the regeneration step of LNT cycling experiments and in practice [26,36–38]. The regeneration gas stream included a mixture of CO and H_2 as reductants and the entire cycle included water, and during the cycling experiments WGS did occur during the regeneration portion of the cycle. The effect of the WGS reaction is the reduction of CO levels in the rich or regeneration gas stream via the following reaction: $CO + H_2O \rightarrow H_2 + CO_2$. Previous work shows that H_2 can more effectively reduce trapped NO_X than can CO at lower temperatures [26,39], thus the more H_2 available as a reductant the more efficient the entire process is. This is also evident based on the data listed in Table 4. The WGS extent is shown in Table 6 at the five temperatures used during the long cycling experiments. The WGS data were obtained from the CO levels at the end of the regeneration phase of the 3rd long cycle. Since high extents of WGS would ultimately help reduction, as H_2 is a better reductant better than CO, it would be ideal to have high extents of WGS at all temperatures, but especially at lower temperatures. The data show that the WGS extent increased with an increase in temperature, but dropped between 463 and 550 °C. At high temperatures (463 and 550 °C) there was little storage and still little reduction demonstrating that although more H_2 was available for better reduction it did not overcome the fact that there is too little nitrate stability at those high temperatures and thus rapid release of NO_X. At 200 °C there was insignificant WGS activity. It is important to note that CO can reduce NO_X directly via $2CO + NO \rightarrow N_2 + CO_2$ and indirectly via the WGS reaction. Thus, it is difficult to confirm which route dominates at 288 and 375 °C. The trend observed here matches that previously observed over the Pt-based catalyst [19], although the values attained with the perovskite sample are lower.

3.4. Oxygen storage capacity (OSC)

Commercial LNT catalysts can contain ceria, which acts as an oxygen storage component. During the regeneration phase of the cycling experiments, the reductants, and intermediate NH_3, can react with the ceria, reducing it, and thereby decrease the amount of available reductant for regeneration and NO_X reduction. This is especially critical at high temperatures, where nitrate decomposition is rapid and a lack of reductant leads to substantial NO_X release. Since the amount of O_2 stored can play a significant role in the regeneration phase, the OSC of the perovskite LNT catalyst was quantified via CO consumption experiments to evaluate the possibility of OSC competition over this system. The experiment was conducted on a cleaned catalyst and in cycles. The catalyst was exposed to a lean gas stream consisting of 10% O_2, 5% CO_2, and a balance of N_2 for 60 s, and then the gas was switched to the rich gas stream consisting of 5% CO_2, 1% CO and a balance of N_2 for 90 s. H_2O was not included in this experiment in order to eliminate the WGS effect. Thirty cycles were completed in order to achieve/guarantee cycle-to-cycle stability. The outlet CO concentrations were used to calculate the amount of O_2 being consumed. Table 6 lists the results from this experiment and shows that the amount of O_2 stored increased with increasing temperature. Clearly there is a substantial amount of OSC, for example 0.44 mmol O_2 stored compared to that of NO_X trapped, 0.035 mmol, at 550 °C. These data show that there will be competition for the reductants between surface oxygen and nitrate decomposition or NO_X reduction. This is true for all temperatures (with different extents of OSC and therefore competition).

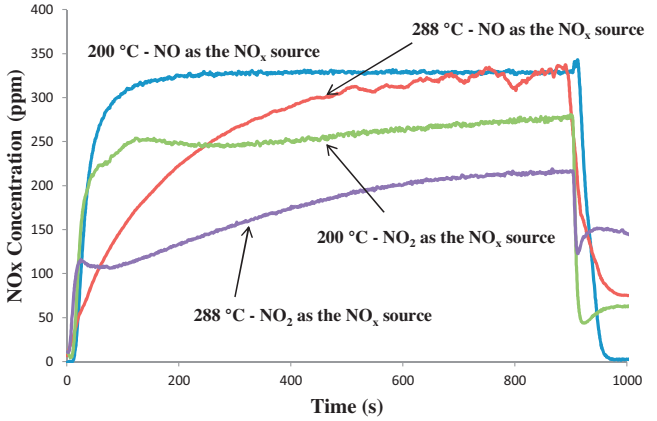

Fig. 10. NO + NO_2 (NO_X) concentration profile at 200 and 288 °C with NO as the NO_X source and 200 and 288 °C with NO_2 as the NO_X source. 300 ppm NO or NO_2, 10% O_2, 5% CO_2, 5% H_2O, balance N_2 at 30,000 h^{-1} space velocity.

3.5. NO_2 as the NO_X source

Literature evidence shows that typical LNT catalysts can trap NO_2 more easily than NO. This includes rates of trapping as well as extents [5–9,19,20]. In testing the perovskite-based sample, using NO_2 as the NO_X source rather than NO also significantly increased the amount of total NO_X trapped, as observed by comparing Figs. 6 and 10, and in comparing the values in Table 7. For example, at 200 °C when the NO_X source was NO or NO_2, 35 and 178 μmol of NO_X were trapped, respectively, and at 288 °C, 137 μmol and 353 μmol of NO_X were trapped, respectively. These results follow the same trends observed with Pt-based LNT catalysts, where limiting factors at low temperatures are NO oxidation and nitrate diffusion [21], as well as the increased NO_2 gas-to-solid phase equilibrium [28]. Based on the NO oxidation results, showing that NO oxidation did occur at these lower temperatures when only NO was in the inlet stream, it is likely that it is the NO_2 gas-to-solid equilibrium that is the limiting factor. NO oxidation was

Table 7
Long cycle storage and reduction performance results using NO as the NO_X source: 300 ppm NO_2, 10% O_2, 5% CO_2, 5% H_2O and a balance of N_2 in the lean phase; 625 ppm CO, 375 ppm H_2, 5% CO_2, 5% H_2O and a balance of N_2 rich phase.

Temperature (°C)	NO_2 as NO_X source NO_X trapped (μmol)	NO as NO_X source NO_X trapped (μmol)	NO_2 as NO_X source NO_X trapped – at 20% BT	NO as NO_X source NO_X trapped – at 20% BT
200	178	135	35	21
288	353	137	67	56

occurring, so it is not solely NO oxidation limiting, and with NO_2 available, the diffusional barrier could be overcome via disproportionation at sites not proximal to the oxidation sites. Of course, this is directly correlated to NO oxidation, the source of NO_2 when only NO is added to the inlet stream.

4. Conclusions

A perovskite-based LNT catalyst was studied, which contained no Pt, but did contain Pd and Rh as part of the formulation. The NO oxidation kinetic study shows that the orders in NO, O_2 and NO_2 were 1.13 ± 0.25, 1.06 ± 0.06, and -1.01 ± 0.26, respectively. The activation energy was found to be 82 ± 11 kJ/mol for the fully formulated perovskite catalyst and 81 ± 11 kJ/mol for the bare perovskite catalyst. In terms of LNT performance, low temperature activity was limited by NO oxidation, surface diffusion or the NO_2 gas-to-solid equilibrium and high temperature performance was limited by nitrate/nitrite stability. Using NO_2 in the inlet stream proved to significantly enhance trapping ability. OSC was significant and therefore will contribute to reductant consumption competition between stored O_2 and stored NO_X. In comparing this perovskite-based catalyst to a Pt-based catalyst, most of the reaction chemistry observed was the same. However, the data suggest that the diffusion limitation was stronger on the perovskite, at low temperature regeneration was not a limiting factor for trapping and that OSC consumption was initially inhibited by the presence of nitrates on the surface; all which differ from previous observations using a Pt-based LNT.

Acknowledgements

The authors would like to thank the Natural Science and Engineering Research Council and General Motors for their financial support of this project.

References

[1] N. Miyoshi, S. Matsumoto, K. Katoh, T. Tanaka, J. Harada, N. Takahashi, K. Yokota, M. Sgiura, K. Kasahara, SAE Technical Paper Series 950809, 1995.
[2] N. Takahashi, H. Shinjoh, T. Iijima, T. Suzuki, K. Yamazaki, K. Yokota, H. Suzuki, N. Miyoshi, S. Matsumoto, T. Tanizawa, T. Tanaka, S. Tateishi, K. Kasahara, Catalysis Today 27 (1996) 63.
[3] W.S. Epling, J. Parks, G. Campbell, A. Yezerets, N. Currier, L. Campbell, Catalysis Today 96 (2004) 21.
[4] W.S. Epling, L. Campbell, A. Yezerets, N. Currier, J. Parks, Catalysis Review 46 (2004) 163.
[5] D.H. Parker, B. Koel, Journal of Vacuum Science and Technology A 8 (1990) 2585.
[6] F. Rodrigues, L. Juste, C. Potvin, J.F. Tempère, G. Blanchard, G. Djéga-Mariadassou, Catalysis Letters 72 (2001) 59.
[7] S. Hodjati, K. Vaezzadeh, C. Petit, V. Pitchon, A. Kiennemann, Catalysis Today 59 (2000) 323.
[8] S. Hodjati, C. Petit, V. Pitchon, A. Kiennemann, Journal of Catalysis 197 (2001) 324.
[9] N.W. Cant, M.J. Patterson, Catalysis Today 73 (2002) 271.
[10] C.H. Kim, G. Qi, K. Dahlberg, W. Li, Science 327 (2010) 1624.
[11] J.G. McCarty, H. Wise, Catalysis Today 8 (1990) 231.
[12] H. Arai, T. Yamada, K. Eguchi, T. Seiyama, Applied Catalysis 26 (1986) 265.
[13] R. Spinicci, M. Faticanti, P. Marini, S. De Rossi, P. Porta, Journal of Molecular Catalysis A: Chemical 197 (2003) 147.
[14] F.E. López-Suárez, M.J. Illán-Gómez, A. Bueno-López, J.A. Anderson, Applied Catalysis B: Environmental 104 (2011) 261.
[15] X. He, M. Meng, J. He, Z. Zou, X. Li, Z. Li, Z. Jiang, Catalysis Communications 12 (2010) 165.
[16] R.J. Farrauto, M.C. Hobson, T. Kennelly, E.M. Waterman, Applied Catalysis A: General 81 (1992) 227.
[17] Platinum Today, Web-based Realtime PGM Prices, www.platinum.matthey.com/index.html (Johnson Matthey Precious Metal Marketing).
[18] X. Zhang, H. Li, Y. Li, W. Shen, Catalysis Letters 142 (2011) 118.
[19] W.S. Epling, A. Yezerets, N.W. Currier, Applied Catalysis B: Environmental 74 (2007) 117.
[20] S.S. Mulla, N. Chen, W.N. Delgass, W.S. Epling, F.H. Ribeiro, Catalysis Letters 100 (2005) 267.
[21] J. Segner, W. Vielhaber, G. Ertl, Israel Journal of Chemistry 22 (1982) 375.
[22] B.M. Weiss, E. Iglesia, Journal of Catalysis 272 (2010) 74.
[23] D. Bhatia, R.W. McCabe, M.P. Harold, V. Balakotaiah, Journal of Catalysis 266 (2009) 106.
[24] J. Kwak, D. Kim, T. Szailer, C. Peden, J. Szanyi, Catalysis Letters 111 (2006) 119.
[25] W.S. Epling, A. Yezerets, N. Currier, Catalysis Letters 110 (2006) 143.
[26] M. AL-Harbi, W.S. Epling, Applied Catalysis B: Environmental 89 (2009) 315.
[27] J. Wang, Y. Ji, V. Easterling, M. Crocker, M. Dearth, R.W. McCabe, Catalysis Today 175 (2011) 83.
[28] M. AL-Harbi, W.S. Epling, Catalysis Letters 130 (2009) 121.
[29] I. Nova, L. Lietti, L. Castoldi, E. Tronconi, P. Forzatti, Journal of Catalysis 239 (2006) 244.
[30] A. Amberntsson, H. Persson, P. Engström, B. Kasemo, Applied Catalysis B: Environmental 31 (2001) 27.
[31] T.J. Toops, D.B. Smith, W.S. Epling, J.E. Parks, W.P. Partridge, Applied Catalysis B: Environmental 58 (2005) 255.
[32] V. Medhekar, V. Balakotaiah, M. Harold, Catalysis Today 121 (2007) 226.
[33] J.A. Pihl, J.E. Parks II, C.S. Daw, T.W. Root, SAE Technical Paper Series 2006-01-3441.
[34] L. Cumaranatunge, S.S. Mulla, A. Yezerets, N.W. Currier, W.N. Delgass, F.H. Ribeiro, Journal of Catalysis 246 (2007) 29.
[35] P. Forzatti, L. Lietti, I. Nova, Energy and Environmental Science 1 (2008) 236.
[36] J.A. Botas, M.A. Gutiérrez-Ortiz, M.P. González-Marcos, Applied Catalysis B: Environmental 32 (2001) 243.
[37] L. Limousy, H. Mahzoul, J.F. Brilhac, F. Garin, G. Maire, P. Gilot, Applied Catalysis B: Environmental 45 (2003) 169.
[38] Y. Li, S. Roth, J. Dettling, T. Beutel, Topics in Catalysis 16/17 (2001) 139.
[39] T. Szailer, J.H. Kwak, D.H. Kim, J.C. Hanson, C.H.F. Peden, J. Szanyi, Journal of Catalysis 239 (2006) 51.